JACS Au
AN OPEN ACCESS JOURNAL OF THE AMERICAN CHEMICAL SOCIETY

pubs.acs.org/jacsau
Article

Selective [3 + 2] C−H/C−H Alkyne Annulation via Dual (Distal) $C_{(\beta,\,\delta)}$−H Bond Activation Relay: A Novel Therapeutic Quinazolone-Tethered Benzofulvenes for Oral Cancer

Dinesh Parshuram Satpute,[§] Garvita Narang,[§] Harshal Rohit, Jagdish Manjhi, Divita Kumar, Sangita Dattatray Shinde, Shyam Kumar Lokhande, Priyanka Patel Vatsa, Vinal Upadhyay, Shivkanya Madhavrao Bhujbal, Amit Mandoli,* and Dinesh Kumar*

Cite This: JACS Au 2024, 4, 4474−4487

Read Online

ACCESS | Metrics & More | Article Recommendations | Supporting Information

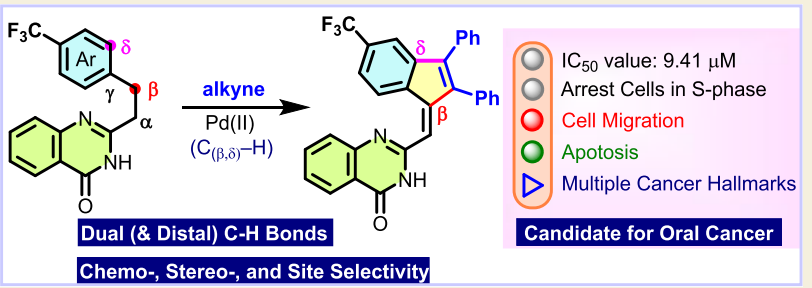

ABSTRACT: In contrast to proximal C−H bond activations, distal C−H bond activation is fundamentally more challenging and requires distinctly specialized directing partners or techniques. In this context, we report an unprecedented dual (distal) *β*-C(benzylic)−H and *δ*-C(aryl)−H bond activation relay protocol for the chemo-, regio-, and stereoselective construction of heterocycle-tethered benzofulvenes via [3 + 2] CH/CH-alkyne annulation under palladium catalysis. The protocol overrides the more favorable [4 + 2] CH/NH annulation and does not follow the vinylic C−H bond activation pathway. Mechanistic studies provide insight into the favored cyclopalladation of key intermediates (resulting from *β*-C(benzylic)−H bond cleavage) through relay *δ*-C(aryl)−H cleavage (vs N−H cleavage) prior to reductive elimination, which is the key to desired annulation. The synthesized new chemical entities (NCEs) constitute a novel scaffold with favorable anticancer activity against oral squamous cell carcinoma (OSCC). Detailed biomolecular studies, including RNA-sequencing and analysis, indicate that these compounds (**4e** and **4w**) arrest the cell cycle at the S-phase and target multiple cancer hallmarks, such as the activation of apoptotic pathways and impairment of mitochondrial activity simultaneously, suggesting their chemotherapeutic potential for oral cancer by addressing the complexity and adaptability of cancer cells in chorus.

KEYWORDS: *distal C−H bond activation, Pd-catalysis, NHC ligand, alkyne annulation, quinazolone-tethered benzofulvenes, oral cancer*

INTRODUCTION

The early phase of drug discovery depends largely on the supply of new chemical entities (NCEs) to ensure the assessment of library compounds (including SAR studies) to acquire the potential hit/lead compounds.[1−3] As a result, the development of novel synthetic approaches, including both early and late-stage diversification strategies, to generate NCEs is extremely promising.[4] Over time, a general consensus has emerged in academia and industry over the sustainability and efficacy of organic synthesis via step- and atom-economic processes, along with the demand for environmental safety.[5,6] In this context, the C−H bond activation strategy that negates the need for substrate-functionalization is highly desirable and rewarding.[7] Toward this end, outstanding development has been observed,[8−11] particularly the directed *ortho* (proximal) C−H bond activation,[12−16] leading to a diverse array of products with a multitude of applications ranging from materials to medicine.[17−20]

In recent years, distal (remote) C−H bond activation has emerged as a promising approach for the hitherto difficult synthesis and modifications of many organic frameworks, thereby expanding the range of synthetic possibilities.[21−24] Such approaches are particularly useful for selective functionalizations and late-stage manipulations of complex organic molecules, such as pharmaceuticals and natural products,

Received: September 2, 2024
Revised: September 28, 2024
Accepted: October 1, 2024
Published: October 11, 2024

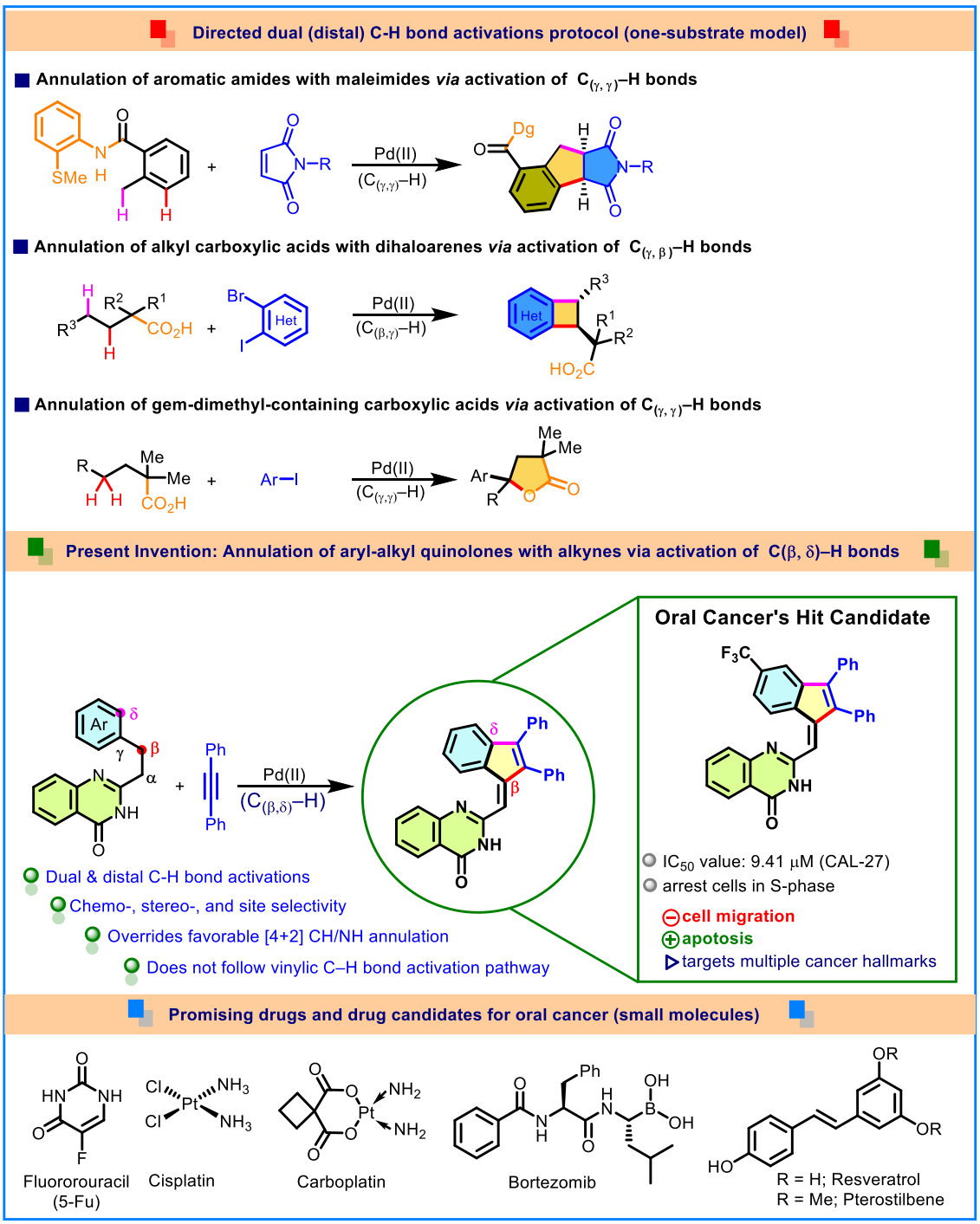

Figure 1. Reported dual (distal) C−H bond activation protocols and the present invention.

amino acids, and macromolecular templates, via sp2 (including *meta*- and *para*−C−H functionalization of arenes) and sp3 C−H bond activation strategies.[25−28] Furthermore, advances in catalyst (and ligand) design have resulted in excellent site-selectivity, allowing for precise functionalizations of distal C−H bonds in molecules with numerous C−H sites having similar electronic and steric preferences using template-directed, transient-directing groups, nondirected, noncovalent interactions, and other approaches.[29−34] Overall, distal C−H bond activation provides new and unique reactivity patterns, allowing the synthesis of novel chemical frameworks that would be difficult to acquire using typical synthetic methods.

Contrasting proximal C−H bond activation, distal C−H bond activation is fundamentally more challenging and, thus, less explored and requires distinctly specialized techniques. Reaching out to the distal positions requires innovative strategies, including but not limited to the intermediacy of larger metallacycles (thermodynamically unfavorable), the specialized directing groups, including the transient directing group, favorable substrate preparations, etc.[25−34] Despite the noticeable progress in the area, the construction of carbo-(hetero)cycles via dual (distal) C−H bond activation constitutes a prime challenge and very limited progress has been taking place.[35−37] In this context, Chatani et al.

https://doi.org/10.1021/jacsau.4c00802
JACS Au 2024, 4, 4474−4487

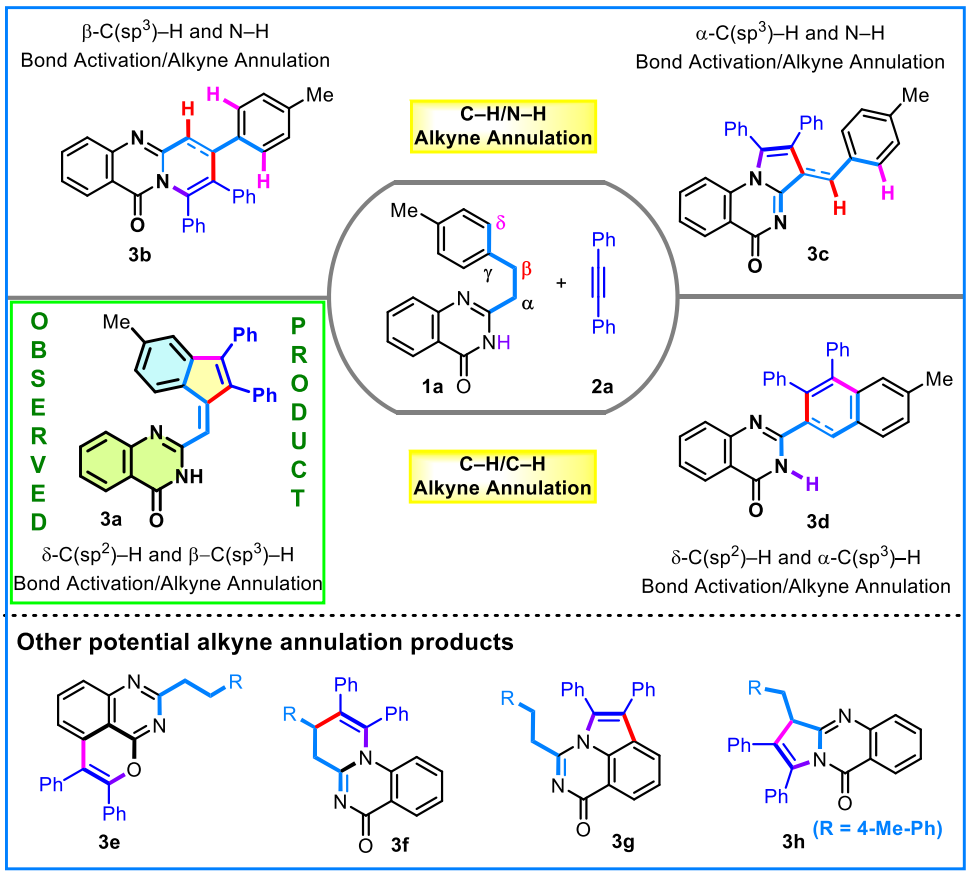

Figure 2. Expected and observed products via annulation of **1a** with **2a**.

developed an elegant annulation of aromatic amides with maleimides via the activation of dual γ-C−H bonds in the presence of a 2-methylthiophenyl amide directing group.[35] In a remarkable finding, Yu et al. discovered a Pd-catalyzed dual $C_{(\gamma,\beta)}$−H activation of adjacent methylene units in carboxylic acids to yield benzocyclobutene (BCB) scaffolds via [2 + 2] benzannulation employing dihaloarenes.[36] The Yu lab further reported a 2-fold $C_{(\gamma,\gamma)}$−H activation protocol with gem-dimethyl-containing carboxylic acids to construct γ-arylated γ-lactones under Pd-catalysis using L,X-type carboxpyridone ligand[37] (Figure 1).

To the best of our knowledge, we report for the first time an unprecedented dual δ-C(aryl)−H and β-C(benzylic)−H bond activation relay protocol for the chemo-, regio-, and stereoselective construction of heterocycle-tethered benzofulvenes[38−40] via [3 + 2] alkyne annulation reactions under palladium catalysis. The mechanistic study highlights the favored cyclopalladation of key intermediates (resulting from β-C(benzylic)−H bond cleavage) through relay δ-C(aryl)−H cleavage (vs N−H cleavage) prior to reductive elimination is the key to desired annulation. The synthesized NCEs constitute a novel scaffold with favorable anticancer activity against oral squamous cell carcinoma (OSCC). Detailed biomolecular studies, including RNA-sequencing and analysis, indicate that these compounds (**4e** and **4w**) arrest the cell cycle at the S-phase and target multiple cancer hallmarks simultaneously, suggesting their chemotherapeutic potential for oral cancer by addressing the complexity and adaptability of cancer cells in chorus.

RESULTS AND DISCUSSION

Method Development

We choose 2-(4-methylphenethyl)quinazolin-4(3*H*)-one **1a** and diphenylacetylene **2a** as a model substrate, and the possible annulation outcome reveals several potential products (**3a−3h**) via heteroatom assistance (Figure 2). The study began with the investigation of ligands (phosphines, bisphosphines, NHCs, and bipyridines) for the reaction involving the treatment of **1a** with **2a** in the presence of catalytic $PdCl_2$ and stoichiometric oxidant $Cu(OAc)_2{\cdot}H_2O$ in 1,4-dioxane under heating conditions. While no product(s) formation was observed using pyridine ligands, the formation of **3a** (NMR, HRMS, single X-ray crystal) was obtained in XPhos (17%) and RuPhos (18%). Other tested phosphines were found to be ineffective in yielding any annulation product(s). The evaluation of NHC ligands was fruitful; the SIPr·HCl was found to be most promising, with an improved yield of **3a** (28%) (Figure 3A). These preliminary results demonstrating unprecedented but highly selective oxidative [3 + 2] C−H/C−H alkyne annulation to make **3a** formed the basis for further explorations.

Subsequently, the other Pd(II) and Pd(0) sources were examined. An improved yield of **3a** (39%) was obtained in $Pd(OAc)_2$. The other tested Pd catalysts were either inferior or ineffective (Figure 3A). A survey of solvents showed that the reaction is solvent sensitive (see SI). While only traces of **3a** formation were observed in DMF, DMSO, DCE, MeCN, and $MeNO_2$, the other tested solvents (PhMe, 1,4-dioxane, THF, and *N*-methyl-2-pyrrolidone (NMP)) were found to be compatible with yields ranging from 11 to 51%. *N*-methyl-2-

https://doi.org/10.1021/jacsau.4c00802
JACS Au 2024, 4, 4474−4487

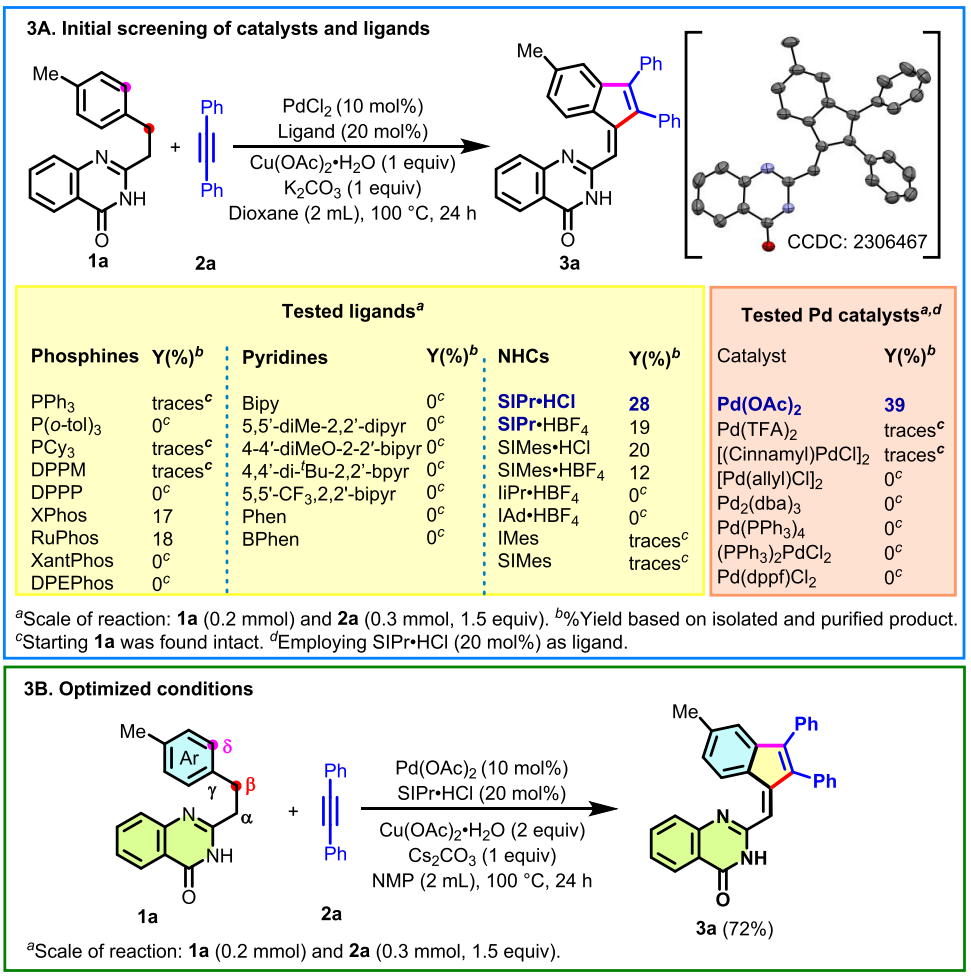

Figure 3. Method development: (A) screening of the ligands and palladium catalysts; (B) optimized conditions.

pyrrolidone (NMP) was found to be the most efficient solvent, providing the highest yield of **3a** (51%) (see SI). Tested catalysts derived from other transition metals (Rh, Ru, Ir, Ni, Mn, and Co) were found to be ineffective (see SI). We further examined different organic and inorganic oxidants, and $Cu(OAc)_2{\cdot}H_2O$ was found to be optimal (see SI). The inclusion of Cs_2CO_3 in place of K_2CO_3 improved the yield significantly, with a 62% isolated yield of **3a** (see SI). A full optimization study revealed that the use of 10 mol % of $Pd(OAc)_2$ and SIPr·HCl (20 mol %) with $Cu(OAc)_2{\cdot}H_2O$ (2 equiv) in NMP at 100 °C was optimal with 72% isolated yield of **3a** (Figure 3B, and see SI). A series of control experiments were performed. In the absence of any one of the reaction components, the reaction failed to yield **3a** (see SI).

Substrate Scope

The scope of the [3 + 2] C−H/C−H alkyne annulation was examined next (Figure 4). The effect of substitution on the phenyl ring was tested first. Electronically different 2-phenethylquinazolin-4(3*H*)-ones reacted well with **2a** to form corresponding *E*-benzofulvenes (**3a**, **4a**−**4f**, **4q**−**4u**) in good to moderate yields. Subsequently, different internal alkynes were tested and found to be compatible under the reaction conditions (**4h**−**4p**) to yield desired benzofulvenes with promising yields and selectivity. Unsymmetrical internal alkynes, 1-ethyl-4-((4-methoxyphenyl)ethynyl)benzene and 1-butynylbenzene, were found to be well-suited with regioselective formation of **4n** (69%, single X-ray crystal) and **4o** (68%, single X-ray crystal), respectively. In contrast, dialkyl alkynes and terminal alkynes failed to yield the product under reaction conditions. The substitutions on the core quinazolone ring were tolerated well with good yields of the desired products (**4q**−**4u**). The corresponding thieno[3,2-*d*]-pyrimidin-4(3*H*)-one and benzofuro[3,2-*d*]pyrimidin-4(3*H*)-one were found compatible, yielding **4v** and **4w**, respectively, with good yield and selectivity. Looking forward to the substrate scope, it is evident that the protocol offers good functional group tolerance as the halogens (−F, −Cl, −Br), electron releasing group (−OMe), electron-withdrawing group ($-CF_3$), and ester ($-CO_2Me$) functionalities were tolerated well without significant reduction in the product yields. Further, piperonyl containing **1a** was found to be compatible with a good yield of product **4f**. Pleased to note that the naphthyl analogue of **1a** resulted in the desired product **4g** with good yield (70%) and stereoselectivity (single X-ray crystal).

Mechanistic Investigation

In order to gain mechanistic insight into this distal [3 + 2] C−H/C−H-alkyne annulation, systematic experiments were proposed and conducted under optimized conditions (Figure 5). First, we examined the essence of heteroatom assistance and the scope of directing partners. No annulation product(s) were observed by the treatment of alkyne **2a** with 1,2-diphenylethane **5a**, 2-phenethylpyridine **5b** or 2-phenethylpyrimidine **5c**, or 2-phenethyl benzothiazole **5d** or 2-phenethyl

https://doi.org/10.1021/jacsau.4c00802
JACS Au 2024, 4, 4474−4487

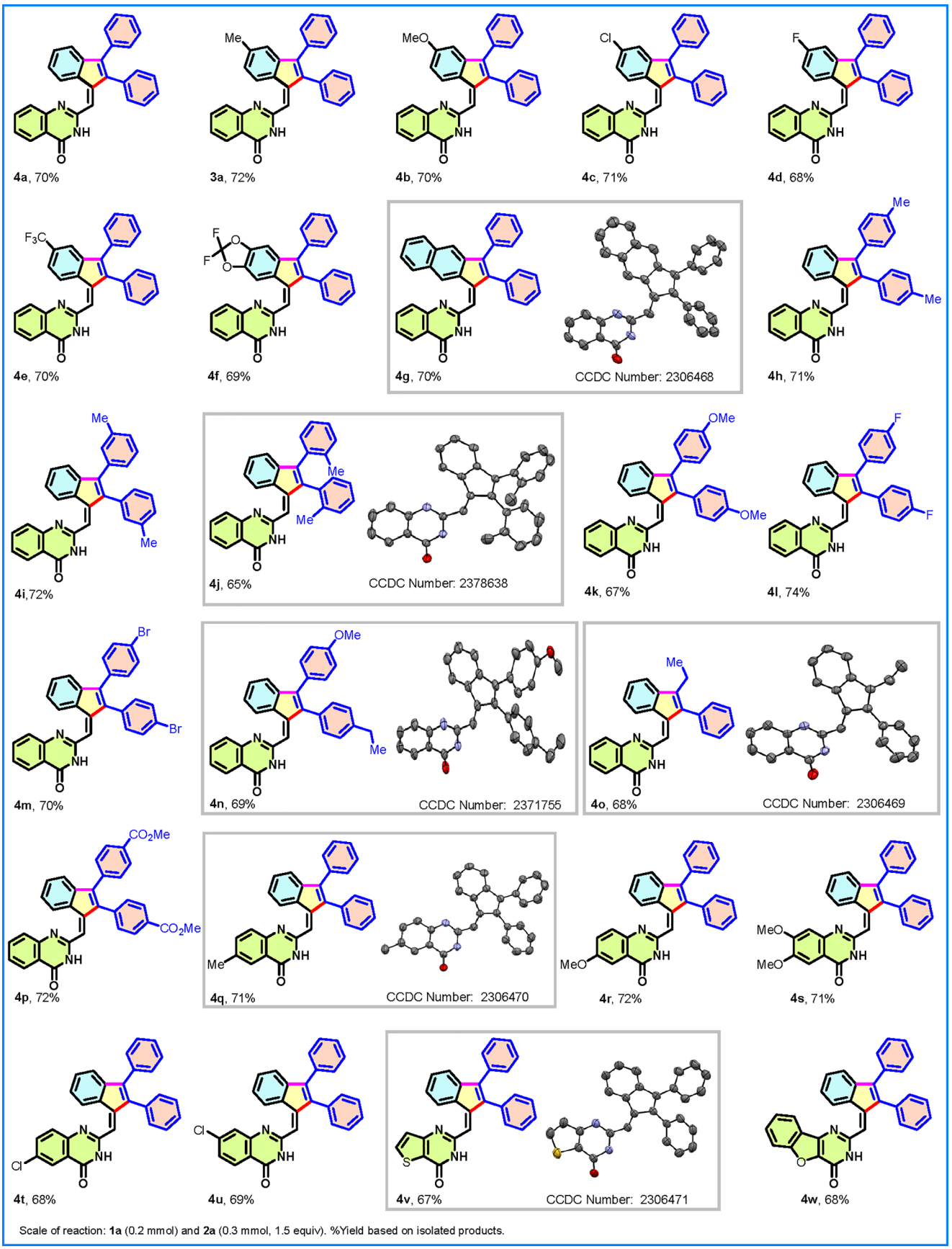

Figure 4. Scope of stereoselective construction of heterocycle-tethered benzofulvenes.

https://doi.org/10.1021/jacsau.4c00802
JACS Au 2024, 4, 4474−4487

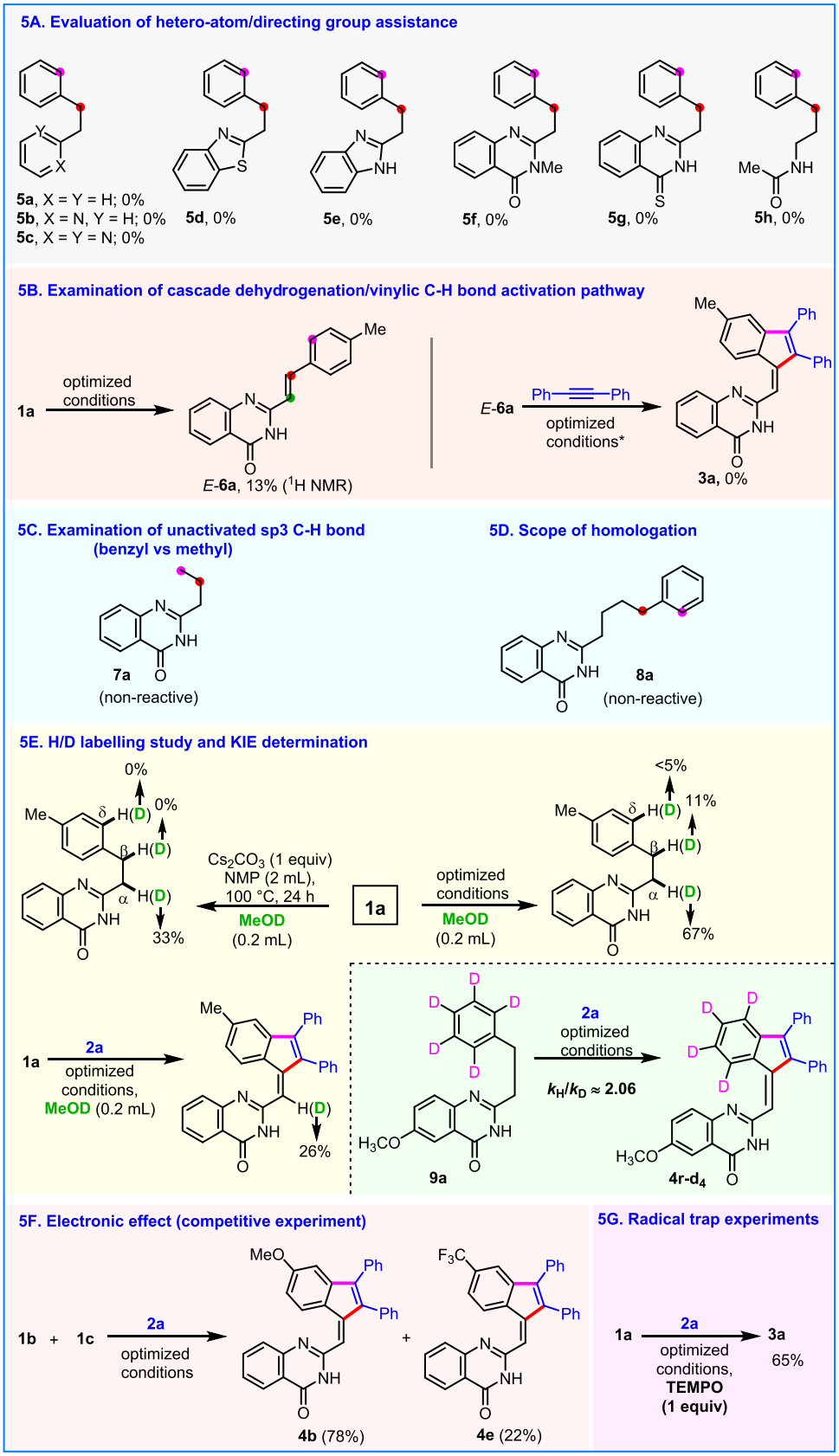

Figure 5. Mechanistic investigations: (A) evaluation of hetero-atom/directing group assistance; (B) examination of cascade dehydrogenation/vinylic C-H bond activation pathway; (C) examination of unactivated sp3 C-H bond (benzyl vs methyl); (D) scope of homologation; (E) H/D labeling study and KIE determination; (F) electronic effect (competitive experiment); (G) radical trap experiments.

https://doi.org/10.1021/jacsau.4c00802
JACS Au 2024, 4, 4474−4487

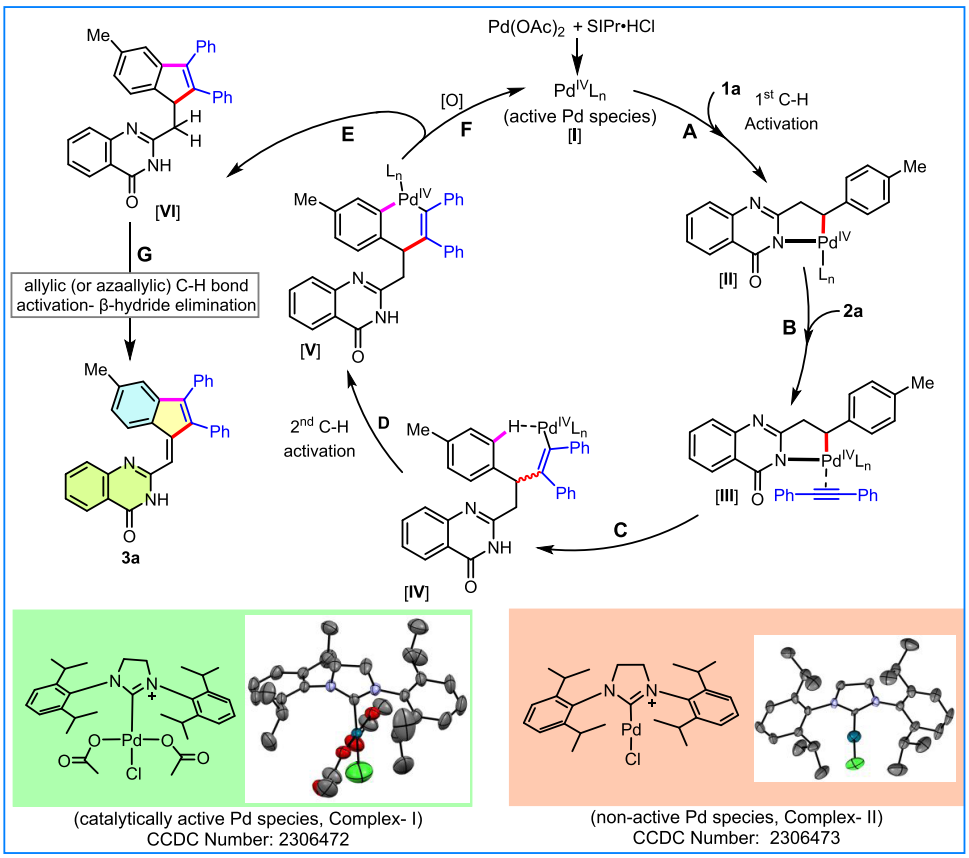

Figure 6. Plausible catalytic cycle depicting the formation of **3a**.

benzimidazole **5e**. Further, N-methylated **1a** (**5f**), thioamide analog **5g**, and corresponding linear arylalkyl amide **5h** were not active under the reaction conditions. These results indicated that the presence of the (NH)-quinazolone type of directing partner is critical for this cyclization reaction (Figure 5A).

Next, we examined the possibility of cascade dehydrogenation/alkyne annulation to make the desired product via vinylic C−H bond activation.[41] Treatment of **1a** under optimized conditions but in absence of alkyne **2a** gave the corresponding 2-styryl quinazolone **6a** (13% ^{1}H NMR), however, preformed **6a** failed to give the **3a** under the reaction conditions. It indicated that the reaction proceeds exclusively via the benzylic C−H bond activation pathway and does not involve the vinylic C−H bond activation (Figure 5B). Replacement of the phenyl moiety with linear alkyl (**7a**) shut down the reaction, further strengthening the operation of the benzylic C−H bond activation pathway (Figure 5C). Homologous chain elongation did not yield the annulation product (**8a**), indicating that the larger palladacycles could not possibly be formed under the reaction conditions (Figure 5D).

To gain the nature of C−H bond cleavage, deuterium-labeling studies were undertaken. Treatment of **1a** with MeOD under optimized conditions but in the absence of alkyne **2a** did not lead to any significant H/D exchange (<5%) at the δ-CH (phenyl ring) but exhibited significant benzylic H/D exchange (11% D). The major site for H/D exchange was α-CH_2 (67% D); however, this process is a nonproductive route. The study further suggested that this α-methylene H/D exchange is also base (and heat) induced, as it proceeds in the absence of the catalyst/ligand/oxidant as well. In the presence of alkyne **2b**, annulation proceeded with the incorporation of deuterium at the exocyclic C=C bond (26% D) (Figure 5E).

The transformation of **1a** to **3a** reaction involves four C−H bond cleavages (two $C_{(\beta)}$−H bond, one $C_{(\delta)}$−H bond, one $C_{(\alpha)}$−H bond) wherein one $C_{(\beta)}$−H bond (initial C−H cleavage/cyclopalladation) and $C_{(\delta)}$−H bond (final C−H bond cleavage/cyclopalladation) are involved in the actual annulation reaction. We tried our best to prepare the respective substrates to determine which specific C−H bond cleavage is the rate-determining step. Unfortunately, we were successful in preparing the substrate **9a** only and performed the KIE determination study. A significant kinetic isotope effect ($k_H/k_D \approx 2.06$) was observed, suggesting the distal $C_{(\delta)}$−H cleavage to be the rate-determining step[42] (Figure 5E).

In order to examine the electronic effects of a substituent on the phenyl ring of arylalkyl quinazolones, an intermolecular competition experiment was performed. The treatment of the equimolar mixture of **1b** and **1c** with **2a** under optimized conditions gave **4b** and **4e** in 78 and 22% yields (^{1}H NMR), respectively. This result indicates that the presence of an electron-withdrawing group (in a phenyl system) decreases the substrate reactivity toward the product formation and vice versa (Figure 5F). Finally, a radical trap experiment was performed. When the reaction was carried out in the presence of 1 equiv of TEMPO, **3a** was produced in 65% yield, indicating that the reaction does not proceed through a radical mechanism (Figure 5G).

Toward the end, we have evaluated the catalytic efficiency of both isolated Pd complexes, Complex-I (Pd^{IV}) and Complex-II (Pd^{II}) (single X-ray crystal),[43−48] for the transformation of **1a** to **3a** under optimized conditions, without $Pd(OAc)_2$ and

https://doi.org/10.1021/jacsau.4c00802
JACS Au 2024, 4, 4474−4487

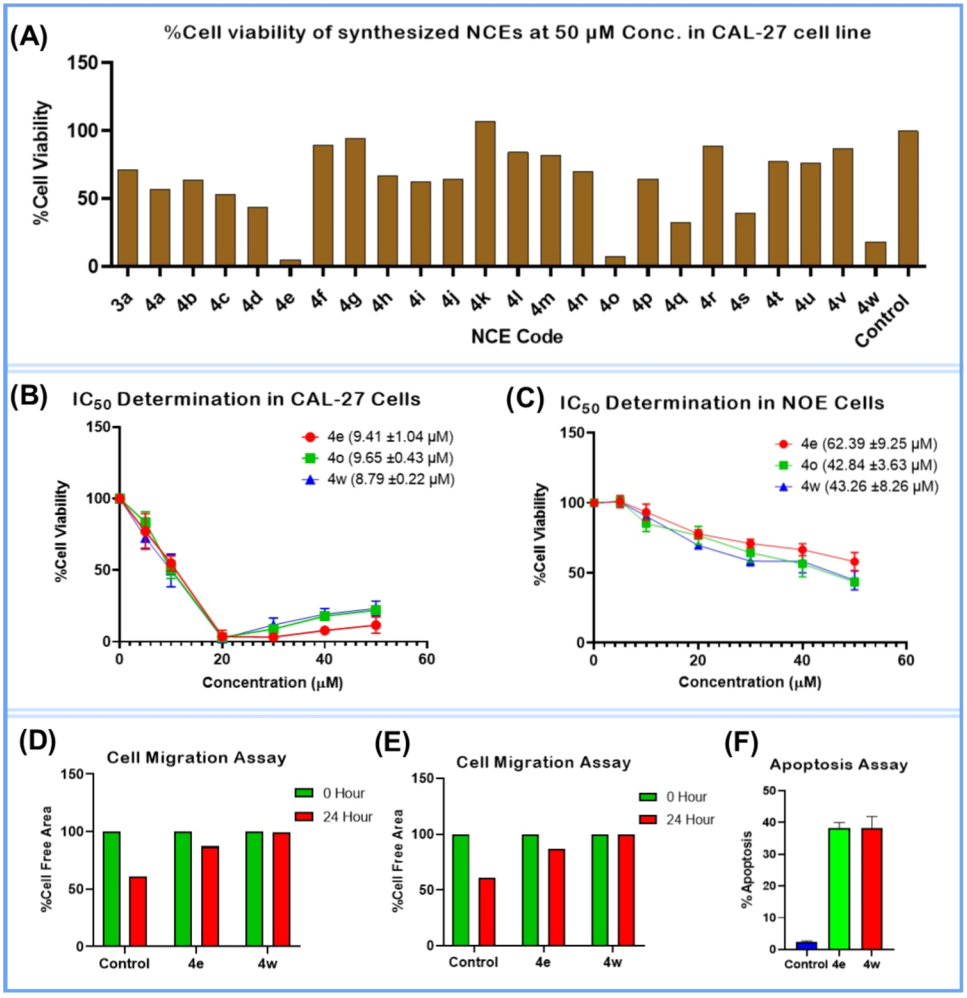

Figure 7. (A) CAL-27 cells were treated with all the synthesized NCEs for 24 h, and the Alamar blue assay was performed to gain insight into %cell viability. The cytotoxicity assay was done in triplicate; plot (B) represents % cell viability in CAL-27 cells; plot (C) represents % cell viability in NOE cells treated with **4e**, **4o**, and **4w**, whereas the two NCEs **4e** and **4w** exhibited selective toxicity (therapeutic index) toward CAL-27 and NOE cells; (D) cell migratory assay showed both the NCEs were effectively arresting the migratory potential of CAL-27 cells; (E) further, cell cycle analysis showed that these compounds **4e** and **4w** arrested the cell cycle at S to G2 phase; (F) apoptosis assay also showed that the treated cells are undergoing apoptosis compared to untreated CAL-27 cells. For further information, see Supporting Data.

SIPr·HCl. While Complex-II proved ineffective, Complex-I catalyzed the reaction, yielding **3a** with a 65% yield (see SI). Given that the reaction did not proceed with $Pd(OAc)_2$ or Complex-II alone, we propose that in situ generated Complex-I (Pd^{IV}) plays a key catalytic role. However, the possibility that Complex-I decomplexes to Pd^{II} species, which could then facilitate the reaction, cannot be ruled out.[49]

Based on mechanistic studies, the proposed catalytic cycle that accounts for product formation is shown in Figure 6. The in situ generated active catalytic species is likely to coordinate with the amide-NH of **1a**, followed by the formation of five-membered palladacycle **II** by the activation of a β-C(benzylic)−H bond, the latter step being reversible C−H cleavage (step A). Alkyne coordination (step B) followed by migratory insertion (step C) would generate intermediate **IV**. Subsequent irreversible δ-C(aryl)−H bond relay cleavage (step D) resulted in the formation of a crucial six-membered palladacycle **V**. Finally, the desired penultimate annulation product was formed through reductive elimination (step E) with the concomitant Cu^{II}-promoted oxidation of Pd^{II} back to the active Pd^{IV} species (step F). The requisite dehydrogenation leading to an exocyclic C═C bond could proceed by the activation of an allylic (or azaallylic) C−H bond followed by β-hydrogen elimination from the resulting Pd-(aza)allyl intermediate (step G).[50] To be noted, the favored cyclopalladation of intermediate **IV** to **V** via δ-C(aryl)−H cleavage (vs N−H cleavage) prior to reductive elimination overrides the conventional CH/NH annulation pathway and yields the desired [3 + 2] CH/CH annulation product. The regioselective annulation (**4o**) using an unsymmetrical alkyl arylacetylene supported the mechanistic hypothesis that benzylic C−H bond activation occurred prior to arene C−H bond activation.

Origin of Selectivity

Considering the amide-NH [−(C═O)−NH−] and heteroatoms (N or O) of **1a** as directing partners, we expect the diverse range of alkyne annulation products (**3a**−**3h**); however, under the reaction conditions, we observed the formation of only **3a**. As we observed the formation of **3a** only, it is evident that under the reaction conditions, only the amide functionality (amide-NH) of **1a** is serving as the directing partner.[41,51] Thus, the cyclization pathways that follow the heteroatom N or O direction for the initial metal insertion and subsequent oxidative addition to form palladacycle are

https://doi.org/10.1021/jacsau.4c00802
JACS Au 2024, 4, 4474−4487

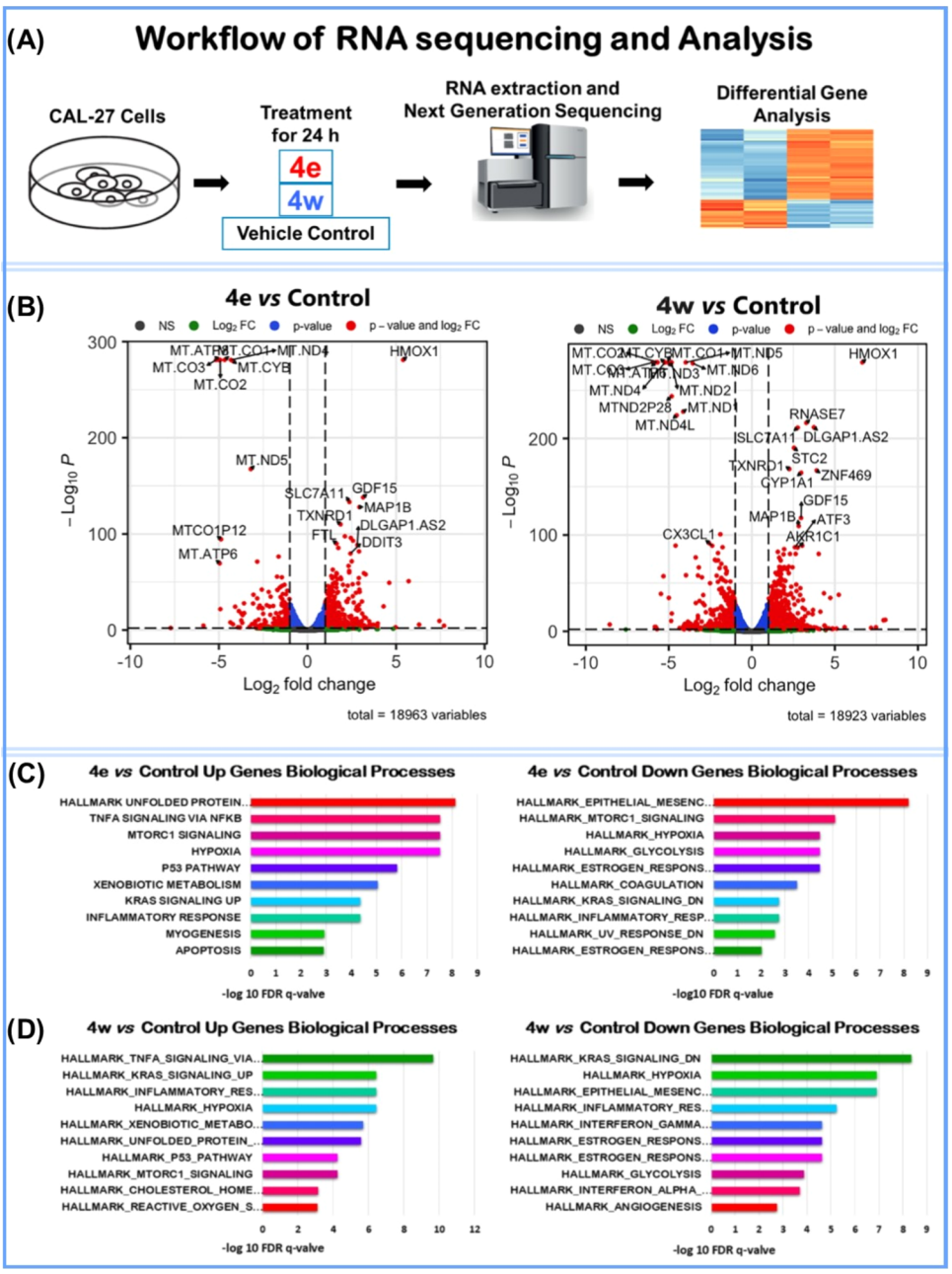

Figure 8. RNA-seq analysis of treated and untreated CAL-27 cells to understand the molecular function of compounds: (A) schematic workflow of RNA sequencing and analysis; (B) volcano plot of the differential gene expression; (C, D) Gene Set Enrichment Analysis (GSEA) results displaying the top 10 significantly enriched hallmark gene sets associated with upregulated and downregulated genes due to both **4e** and **4w**.

nonoperational, and hence, no related products (**3e**, **3f**, and **3g**) were observed. The formation of **3c**, **3d**, and **3h** may follow the amide direction (amide-NH), but the requisite palladacycle is 4-membered, which is otherwise not favorable due to ring strain, thus not leading to such products. The formation of **3a** and **3b** is really compelling in nature; it follows the amide direction (amide-NH) for initial C−H bond cleavage to form common 5-membered palladacycle **II**, which on subsequent alkyne coordination and migratory insertion forms the common key complex **IV**. The complex **IV** will either undergo $C_{(\delta)}$−H bond or N−H bond cleavage to form **3a** (via 6-membered palladacycle) or **3b** (via 7-membered palladacycle), respectively. We believe that the reductive elimination through 6-membered palladacycle leading to **3a** is more facile compared to 7-membered palladacycle (leading to **3b**) as it provides more steric encumbrance.[52] Further, to be noted, the formation of 6-membered palladacycle is more favorable over 7-membered palladacycle due to their ring strain, which further justifies the selectivity of **3a** over **3b**.[53]

Further, from the ligand investigation study, it is evident that NHC ligands are pivotal for this transformation. This could be explained on the basis of the strong σ-donation ability of NHCs to the palladium center, enabling facile oxidative additions (compared to metal-phosphine counterparts).[54−57] Further, such strong σ-donation by NHCs improves the stability of palladium in high oxidation states, which is problematic with typical phosphine ligands due to their facile oxidation to phosphine oxides. The strong metal−carbenic bond of the NHC complex also favors tight binding kinetics,

https://doi.org/10.1021/jacsau.4c00802
JACS Au 2024, 4, 4474−4487

therefore, lessening ligand dissociation. On the other hand, the presence of sterically demanding groups bound to the N atoms enable facile reductive elimination of the product from palladium complexes, as the steric encumbrance is alleviated upon reductive elimination.[58]

Evaluation of Anticancer Activity of Library Compound

In recent years, quinazoline (and fulvene) derivatives have emerged as an important class of cancer chemotherapeutics against a wide range of tumors, including oral cancer.[59−65] The various mechanistic pathways associated with quinazoline-based NCEs include, but are not limited to, the inhibition of protein targets such as kinase,[66−68] lysine methyl transferase,[69] and topoisomerase,[59,70,71] as well as the inhibition of tubulin polymerization,[72,73] vascular endothelial growth factor receptor-2 (VEGFR-2),[74] poly(ADP-ribose) polymerase-1 (PARP-1),[75] and others for their anticancer activities. The FDA has approved many quinazoline derivatives for clinical use, including gefitinib, erlotinib, lapatinib, afatinib, and vandetanib. However, despite advances in chemotherapy (including imaging technology and surgery), oral cancer continues to be characterized by high death rates. According to the GLOBOCAN 2020 report, there were about 177757 deaths and roughly 377713 new cases recorded for cancer of the lip and oral cavity alone.[76,77] Furthermore, the disease's mortality and incidence are expected to climb by 32% by 2040. Thus, recognizing the related mortality and morbidity, as well as the limits of current treatment, the discovery of more effective drugs for oral cancer is of the utmost need.[78] In this context, we investigated the synthesized novel structural framework, benzofulvenes-linked quinazolones, for their possible therapeutic applications in oral cancer.

To identify the most promising anticancer compound(s) among the library (**3a**, **4a**−**4w**) toward oral cancer, we first screened cell viability in the CAL-27[79] oral cancer cell lines at 50 μM (Figure 7A). IC_{50} values of three compounds (**4e**, **4o**, and **4w**) that showed good cell cytotoxicity at 50 μM were determined in CAL-27 (vs normal oral epithelium cell lines, NOE). Compound **4e** showed the best comparative cytotoxicity and cell viability in CAL-27 cancer cells (IC_{50} 9.41 ± 1.04 μM) in comparison to NOE cells (IC_{50} 62.39 ± 9.25 μM) followed by **4o** (IC_{50} 9.65 ± 0.43 vs 42.84 ± 3.63 μM), and **4w** (IC_{50} 8.79 ± 0.22 vs 43.26 ± 8.26 μM; Figure 7B,C). Thus, overall, cytotoxicity results suggested **4e** and **4w** were the top two NCEs exhibiting selective toxicity (therapeutic index) toward the oral cancer cell lines (vs NOE cells), thereby exploring them for further characterization of anticancer properties and biomolecular evaluation at a dose of their respective IC_{50} value (9.41 μM for **4e** and 8.79 μM for **4w**), respectively.

Cell migration and metastasis are one of the core hallmarks of the cancers.[80,81] To examine the effect of the **4e** and **4w** in inhibiting the migratory potential of CAL-27, an in vitro scratch assay was performed.[82] The gap closure measured after 24 h for the **4e** and **4w** treated group was less than the control, suggesting their antimigratory effects against the CAL-27 (Figure 7D and SI). To evaluate the effects of identified NCEs on the cell cycle, CAL-27 cells were treated with **4e** and **4w** for 24 h separately, stained with propidium iodide, and analyzed by flow cytometry (FACS). The cell cycle analysis revealed an increase in the cells of the S-phase and a decrease in the G2-phase, suggesting that the compounds inhibit the S-to-G2 phase transition, thereby arresting the cells in the S-phase (Figure 7E). FACS analysis further revealed that the treated cells were undergoing apoptosis, **4e** (39.526 ± 2.5) and **4w** (40.83 ± 2.74), compared to the untreated CAL-27 cells (2.623333 ± 0.12) (Figure 7F).

To investigate the molecular mechanisms (genes and pathways) underlying the growth inhibition and apoptosis effects induced by compounds **4e** and **4w**, we conducted RNA-seq analyses in untreated and treated CAL-27 cells and compared the global gene expression levels between control and treated cells (Figure 8).[83] Between 50 and 57 million paired end reads were generated in each condition, of which over 95% were mapped to the human genome (hg38). In **4e**-treated cells, 779 differentially expressed (DE) genes were identified (adjusted P value < 0.05 and log2 fold change > 1), of which 550 genes were upregulated, and 229 genes were downregulated (see csv file, SI). Similarly, in **4w**-treated cells, 774 genes were upregulated, and 445 genes were downregulated (see the csv file, SI). Notably, key apoptosis-related genes such as HMOX1, ATF3, DDIT3, and BCL11B were significantly upregulated upon treatment with both compounds, suggesting both **4e** and **4w** activate apoptotic pathways in CAL-27 cancer cells (Figure 8B), thereby also validating the apoptosis seen by FACS analysis. In contrast, several genes associated with mitochondrial OXPHOS system functioning, such as MT-ATP6, MT-CO2, etc., were among the top downregulated with the treatment of both compounds, indicating impaired mitochondrial activity following the treatment with both compounds (Figure 8B).

Gene Set Enrichment Analysis (GSEA) of the upregulated genes after the treatment with **4e** and **4w** revealed the enrichment of gene sets related to apoptosis and the p53 pathway, suggesting that the compounds activate pathways involved in regulating cell growth and apoptosis (Figure 8C,8D, left). In contrast, the downregulated genes were enriched in hallmark gene sets associated with cancer-relevant pathways such as glycolysis, inflammatory response, and epithelial-mesenchymal transition (EMT) (Figure 8C,D, right).

CONCLUSIONS

In conclusion, we report a novel C−H bond activation relay chemistry leading to chemo-, regio, and stereoselective construction of benzofulvenes via dual (distal) $C_{(\beta,\delta)}$-H bond activations-alkyne annulation strategy under palladium catalysis. Surprisingly, more favorable [4 + 2] C−H/NH alkyne annulation products were not observed. The protocol overrides the conventional C−H/N-H annulation pathways and does not follow the pedestrian vinylic C−H bond activation pathway. Mechanistic studies' insight into the favored cyclopalladation via δ-C(aryl)−H cleavage (vs N−H) prior to reductive elimination is a key to success. Further, we have demonstrated the potent anticancer activity of the selected NCEs (**4e**, **4w**) in the oral cancer cell line (CAL-27) wherein these compounds arrest the cell cycle at the S-phase, inhibit cell migration, and induce apoptosis. The RNA-seq analysis revealed that both NCEs (**4e** & **4w**) target multiple cancer hallmarks such as activation of apoptotic pathways (via upregulation of apoptosis-related genes like HMOX1, ATF3, DDIT3, & BCL11B), impairment of mitochondrial activity (via downregulation of genes associated with mitochondrial OXPHOS system functioning, such as MT-ATP6, MT-CO2, etc.) simultaneously, suggesting their chemotherapeutic

https://doi.org/10.1021/jacsau.4c00802
JACS Au 2024, 4, 4474−4487

potential for oral cancer by addressing the complexity and adaptability of cancer cells in chorus.

METHODS

General Procedure for the Synthesis of the Quinazolone-Tethered Benzofulvenes via [3 + 2] C−H/C−H Alkyne Annulation

Into an oven-dried 1-dram scintillation vial equipped with a magnetic stir-bar, palladium(II) acetate [$Pd(OAc)_2$] (4.5 mg, 0.02 mmol, 10 mol %), 1,3-bis(2,6-diisopropylphenyl)imidazolinium chloride [SIPr·HCl] (17 mg, 0.04 mmol, 20 mol %), $Cu(OAc)_2·H_2O$ (80 mg, 0.4 mmol, 2 equiv), Cs_2CO_3 (65 mg, 0.2 mmol, 1 equiv) followed by **1a** (53 mg, 0.2 mmol, 1 equiv) and **2a** (53 mg, 0.3 mmol, 1.5 equiv) were dissolved in 2 mL of NMP in a glovebox. The vial was sealed with a screw cap with the PTFE liner, transferred out of the glovebox, and stirred at 100 °C for 24 h. Upon completion, the reaction was cooled to ambient temperature, diluted with ethyl acetate, and passed through the Celite bed. The workup was done using water/brine and ethyl acetate. The organic layer was dried over Na_2SO_4 and concentrated in vacuo and purified by column chromatography (solvent system: hexane−ethyl acetate) to afford analytically pure (*E*)-2-(5-methyl-2,3-diphenyl-1*H*-inden-1-ylidene)methylquinazolin-4(3*H*)-one **3a**.

ASSOCIATED CONTENT

Supporting Information

The Supporting Information is available free of charge at https://pubs.acs.org/doi/10.1021/jacsau.4c00802.

The detailed experimental procedure, compound characterization data, related mechanistic study, and bioevaluation of compounds (PDF)

4e DF genes and **4w** DF genes (XLSX)

Accession Codes

Crystallographic data for the structures reported in this article have been deposited at the Cambridge Crystallographic Data Centre (CCDC), having CCDC numbers 2306467 (**3a**), 2306468 (**4g**), 2378638 (**4j**), 2371755 (**4n**), 2306469 (**4o**), 2306470 (**4q**), 2306471 (4v), 2306472 (Pd Complex-I), and 2306473 (Pd Complex-II).

AUTHOR INFORMATION

Corresponding Authors

Amit Mandoli − *Department of Biotechnology, National Institute of Pharmaceutical Education and Research (NIPER) − Ahmedabad, Gandhinagar 382355 Gujarat, India*; Email: amitmandoli@niperahm.res.in

Dinesh Kumar − *Department of Medicinal Chemistry, National Institute of Pharmaceutical Education and Research (NIPER) − Ahmedabad, Gandhinagar 382355 Gujarat, India*; orcid.org/0000-0003-2680-881X; Email: dkchem79@gmail.com, dineshk@niperahm.ac.in

Authors

Dinesh Parshuram Satpute − *Department of Medicinal Chemistry, National Institute of Pharmaceutical Education and Research (NIPER) − Ahmedabad, Gandhinagar 382355 Gujarat, India*

Garvita Narang − *Department of Medicinal Chemistry, National Institute of Pharmaceutical Education and Research (NIPER) − Ahmedabad, Gandhinagar 382355 Gujarat, India*

Harshal Rohit − *Department of Biotechnology, National Institute of Pharmaceutical Education and Research (NIPER) − Ahmedabad, Gandhinagar 382355 Gujarat, India*

Jagdish Manjhi − *Department of Medicinal Chemistry, National Institute of Pharmaceutical Education and Research (NIPER) − Ahmedabad, Gandhinagar 382355 Gujarat, India*

Divita Kumar − *Department of Medicinal Chemistry, National Institute of Pharmaceutical Education and Research (NIPER) − Ahmedabad, Gandhinagar 382355 Gujarat, India*

Sangita Dattatray Shinde − *Department of Medicinal Chemistry, National Institute of Pharmaceutical Education and Research (NIPER) − Ahmedabad, Gandhinagar 382355 Gujarat, India*

Shyam Kumar Lokhande − *Department of Medicinal Chemistry, National Institute of Pharmaceutical Education and Research (NIPER) − Ahmedabad, Gandhinagar 382355 Gujarat, India*

Priyanka Patel Vatsa − *Department of Biotechnology, National Institute of Pharmaceutical Education and Research (NIPER) − Ahmedabad, Gandhinagar 382355 Gujarat, India*

Vinal Upadhyay − *Department of Biotechnology, National Institute of Pharmaceutical Education and Research (NIPER) − Ahmedabad, Gandhinagar 382355 Gujarat, India*

Shivkanya Madhavrao Bhujbal − *Department of Medicinal Chemistry, National Institute of Pharmaceutical Education and Research (NIPER) − Ahmedabad, Gandhinagar 382355 Gujarat, India*

Complete contact information is available at: https://pubs.acs.org/10.1021/jacsau.4c00802

Author Contributions

[§]D.P.S. and G.N. contributed equally. The project was conceptualized by Dinesh Kumar. D.P.S. and G.N. carried out the optimization, chemical synthesis, and mechanistic analysis. Compound synthesis was helped by J.M., Divita Kumar, S.D.S., S.K.L., and S.M.B. All biological and molecular research works were carried out by H.R., P.P.V., V.U., and A.M. A.M. and Dinesh Kumar both worked on this manuscript's writing. The final manuscript was reviewed and approved by all authors. CRediT: **Dinesh Parshuram Satpute** data curation, formal analysis, investigation, methodology; **Garvita Narang** data curation, formal analysis, investigation, methodology, validation; **Harshal Rohit** data curation, formal analysis, investigation; **Jagdish Manjhi** formal analysis, methodology, validation; **Divita Kumar** methodology, validation; **Sangita Dattatray Shinde** methodology, validation; **Shyam Kumar Lokhande** methodology, validation; **Priyanka Patel Vatsa** formal analysis, investigation, validation; **Vinal Upadhyay** formal analysis, investigation, validation; **Shivkanya Madhavrao Bhujbal** methodology; **Amit Mandoli** project administration, resources, software, supervision, validation, visualization, writing - original draft, writing - review & editing; **Dinesh Kumar** conceptualization, data curation, formal analysis, funding acquisition, project administration, resources, software, supervision, validation, visualization, writing - original draft, writing - review & editing.

https://doi.org/10.1021/jacsau.4c00802
JACS Au 2024, 4, 4474−4487

Notes

The authors declare the following competing financial interest(s): This innovation is the subject of an Indian patent application (application number: 202421073889).

■ ACKNOWLEDGMENTS

Authors thank the Department of Pharmaceuticals (DoP), Ministry of Chemical and Fertilizers, and NIPER-Ahmedabad for financial support. Dinesh Kumar gratefully acknowledges the DST-SERB for the award of the Ramanujan Fellowship (File No. SB/S2/RJN-135/2017), Start-up Research Grant (File No. SRG/2020/000658), and Core-Research Grant (CRG/2022/004057). Dinesh Kumar also thanks CSIR-HRDG for CSIR Research Grants (File No. 02(0456)21/EMR-II). A.M. gratefully acknowledges Gujarat State Biotechnology Mission (File No GSBTM/JD(R&D)/618/21-22/1222), and Indian Council of Medical Research (File No: NCD/Ad-hoc/223/2022-2) for the research funding. The authors sincerely acknowledge the Dr. Vijay Thiruvenkatam, IIT Gandhinagar, Gujarat (India), and Mr. Mahesh Shrichand Rathod, University of Hyderabad, Hyderabad (India) for solving the XRD structures.

■ DEDICATION

This work is dedicated to Professor Asit K. Chakraborti (NIPER, SAS Nagar, India) and Professor Gregory R. Cook (Department of Chemistry and Biochemistry, NDSU, Fargo, USA) in recognition of their exceptional mentorship and their invaluable contributions to the field of chemical science.

■ REFERENCES

(1) Lombardino, J. G.; Lowe, J. A. The role of the medicinal chemist in drug discovery—then and now. *Nat. Rev. Drug Discovery* **2004**, *3*, 853−862.
(2) Keserü, G. M.; Makara, G. M. The influence of lead discovery strategies on the properties of drug candidates. *Nat. Rev. Drug Discovery* **2009**, *8*, 203−212.
(3) Bajorath, J.; Peltason, L.; Wawer, M.; Guha, R.; Lajiness, M. S.; Van Drie, J. H. Navigating structure−activity landscapes. *Drug Discovery Today* **2009**, *14*, 698−705.
(4) Bryan, M. C.; Dillon, B.; Hamann, L. G.; Hughes, G. J.; Kopach, M. E.; Peterson, E. A.; Pourashraf, M.; Raheem, I.; Richardson, P.; Richter, D.; Sneddon, H. F. Sustainable practices in medicinal chemistry: current state and future directions. *J. Med. Chem.* **2013**, *56*, 6007−6021.
(5) Matlin, S. A.; Mehta, G.; Hopf, H.; Krief, A. The Role of Chemistry in Inventing a Sustainable Future. *Nat. Chem.* **2015**, *7*, 941−943.
(6) Trost, B. M. The Atom Economy—A search for synthetic efficiency. *Science* **1991**, *254*, 1471−1477.
(7) Dalton, T.; Faber, T.; Glorius, F. C−H Activation: Toward sustainability and applications. *ACS Cent. Sci.* **2021**, *7*, 245−261.
(8) Labinger, J. A.; Bercaw, J. E. Understanding and exploiting C−H bond activation. *Nature* **2002**, *417*, 507−514.
(9) Balcells, D.; Clot, E.; Eisenstein, O. C−H Bond activation in transition metal species from a computational perspective. *Chem. Rev.* **2010**, *110*, 749−823.
(10) Sambiagio, C.; Schönbauer, D.; Blieck, R.; Dao-Huy, T.; Pototschnig, G.; Schaaf, P.; Wiesinger, T.; Zia, M. F.; Wencel-Delord, J.; Besset, T.; Maes, B. U. W.; Schnürch, M. A comprehensive overview of directing groups applied in metal-catalysed C−H functionalization chemistry. *Chem. Soc. Rev.* **2018**, *47*, 6603−6743.
(11) Hartwig, J. F. Evolution of C−H bond functionalization from methane to methodology. *J. Am. Chem. Soc.* **2016**, *138*, 2−24.
(12) Sun, L.; Chen, H.; Liu, B.; Chang, J.; Kong, L.; Wang, F.; Lan, Y.; Li, X. Rhodium-catalyzed atroposelective construction of indoles via C−H bond activation. *Angew. Chem., Int. Ed.* **2021**, *60*, 8391−8395.
(13) Liu, X.-H.; Park, H.; Hu, J.-H.; Hu, Y.; Zhang, Q.-L.; Wang, B.-L.; Sun, B.; Yeung, K.-S.; Zhang, F.-L.; Yu, J.-Q. Diverse *Ortho*-C(Sp2)−H functionalization of benzaldehydes using transient directing groups. *J. Am. Chem. Soc.* **2017**, *139*, 888−896.
(14) Rej, S.; Ano, Y.; Chatani, N. Bidentate Directing Groups: An efficient tool in C−H bond functionalization chemistry for the expedient construction of C−C bonds. *Chem. Rev.* **2020**, *120*, 1788−1887.
(15) Gandeepan, P.; Müller, T.; Zell, D.; Cera, G.; Warratz, S.; Ackermann, L. 3d Transition metals for C−H activation. *Chem. Rev.* **2019**, *119*, 2192−2452.
(16) Ye, J.; Lautens, M. Palladium-catalysed norbornene-mediated C−H functionalization of arenes. *Nat. Chem.* **2015**, *7*, 863−870.
(17) Wencel-Delord, J.; Glorius, F. C−H Bond activation enables the rapid construction and late-stage diversification of functional molecules. *Nat. Chem.* **2013**, *5*, 369−375.
(18) Zhang, J.; Kang, L. J.; Parker, T. C.; Blakey, S. B.; Luscombe, C. K.; Marder, S. R. recent developments in C−H activation for materials science in the center for selective C−H activation. *Molecules* **2018**, *23*, 922.
(19) Baudoin, O. Multiple catalytic C−H bond functionalization for natural product synthesis. *Angew. Chem., Int. Ed.* **2020**, *59*, 17798−17809.
(20) Hagui, W.; Doucet, H.; Soulé, J.-F. Application of palladium-catalyzed C(sp2)−H bond arylation to the synthesis of polycyclic (hetero) aromatics. *Chem* **2019**, *5*, 2006−2078.
(21) Sinha, S. K.; Guin, S.; Maiti, S.; Biswas, J. P.; Porey, S.; Maiti, D. Toolbox for distal c−h bond functionalizations in organic molecules. *Chem. Rev.* **2022**, *122*, 5682−5841.
(22) Dutta, U.; Maiti, S.; Bhattacharya, T.; Maiti, D. Arene diversification through distal C(Sp2)−H functionalization. *Science* **2021**, *372*, 6543.
(23) Shi, H.; Lu, Y.; Weng, J.; Bay, K. L.; Chen, X.; Tanaka, K.; Verma, P.; Houk, K. N.; Yu, J.-Q. differentiation and functionalization of remote C−H bonds in adjacent positions. *Nat. Chem.* **2020**, *12*, 399−404.
(24) Goswami, N.; Bhattacharya, T.; Maiti, D. Transient directing ligands for selective metal-catalyzed C−H activation. *Nat. Rev. Chem.* **2021**, *5*, 646−659.
(25) Das, J.; Dolui, P.; Ali, W.; Biswas, J. P.; Chandrashekar, H. B.; Prakash, G.; Maiti, D. A direct route to six and seven membered lactones via γ-C(Sp 3)−H Activation: a simple protocol to build molecular complexity. *Chem. Sci.* **2020**, *11*, 9697−9702.
(26) Xia, Y.; Wang, J.; Dong, G. Distal-bond-selective C−C Activation of ring-fused cyclopentanones: an efficient access to spiroindanones. *Angew. Chem., Int. Ed.* **2017**, *56*, 2376−2380.
(27) Guillemard, L.; Ackermann, L.; Johansson, M. J. Late-stage *meta*-C−H alkylation of pharmaceuticals to modulate biological properties and expedite molecular optimization in a single step. *Nat. Commun.* **2024**, *15*, No. 3349.
(28) He, G.; Chen, G. A practical strategy for the structural diversification of aliphatic scaffolds through the palladium-catalyzed picolinamide-directed remote functionalization of unactivated C-(Sp^3)-H bonds. *Angew. Chem., Int. Ed.* **2011**, *50*, 5192−5196.
(29) Das, J.; Guin, S.; Maiti, D. Diverse strategies for transition metal catalyzed distal C(Sp^3)−H functionalizations. *Chem. Sci.* **2020**, *11*, 10887−10909.
(30) Zhang, Z.; Tanaka, K.; Yu, J.-Q. Remote site-selective C−H activation directed by a catalytic bifunctional template. *Nature* **2017**, *543*, 538−542.
(31) Leow, D.; Li, G.; Mei, T.-S.; Yu, J.-Q. Activation of remote meta-C−H bonds assisted by an end-on template. *Nature* **2012**, *486*, 518−522.
(32) Bag, S.; Patra, T.; Modak, A.; Deb, A.; Maity, S.; Dutta, U.; Dey, A.; Kancherla, R.; Maji, A.; Hazra, A.; Bera, M.; Maiti, D.

https://doi.org/10.1021/jacsau.4c00802
JACS Au 2024, 4, 4474−4487

Remote *para*-C−H functionalization of arenes by a d-shaped biphenyl template-based assembly. *J. Am. Chem. Soc.* **2015**, *137*, 11888−11891.
(33) Ali, W.; Saha, A.; Ge, H.; Maiti, D. Photoinduced *meta*-Selective C−H Oxygenation of Arenes. *JACS Au* **2023**, *3*, 1790−1799.
(34) Geng, J.; Fang, Z.; Tu, G.; Zhao, Y. Non-directed highly *para*-selective C-H functionalization of TIPS-protected phenols promoted by a carboxylic acid ligand. *Chin. Chem. Lett.* **2023**, *34*, No. 107609.
(35) He, Q.; Chatani, N. Palladium-catalyzed site-selective [3 + 2] annulation via benzylic and meta C−H bond activation. *Angew. Chem., Int. Ed.* **2021**, *60*, 5189−5192.
(36) Yang, J.-M.; Lin, Y.-K.; Sheng, T.; Hu, L.; Cai, X.-P.; Yu, J.-Q. Regio-controllable [2 + 2] benzannulation with two adjacent C(sp3)−H bonds. *Science* **2023**, *380*, 639−644.
(37) Hoque, M. E.; Yu, J.-Q. Ligand-Enabled Double γ-C(sp3)−H Functionalization of aliphatic acids: One-step synthesis of γ-arylated γ-lactones. *Angew. Chem., Int. Ed.* **2023**, *62*, No. e202312331.
(38) Donslund, B. S.; Nielsen, R. P.; Mønsted, S. M. N.; Jørgensen, K. A. Benzofulvenes in trienamine catalysis: stereoselective spiroindene synthesis. *Angew. Chem., Int. Ed.* **2016**, *55*, 11124−11128.
(39) Kosaka, Y.; Kawauchi, S.; Goseki, R.; Ishizone, T. High anionic polymerizability of benzofulvene: new exo-methylene hydrocarbon monomer. *Macromolecules* **2015**, *48*, 4421−4430.
(40) Seltzman, H. H.; Shiner, C.; Hirt, E. E.; Gilliam, A. F.; Thomas, B. F.; Maitra, R.; Snyder, R.; Black, S. L.; Patel, P. R.; Mulpuri, Y.; Spigelman, I. peripherally selective cannabinoid 1 receptor (CB1R) agonists for the treatment of neuropathic pain. *J. Med. Chem.* **2016**, *59*, 7525−7543.
(41) Kumar, D.; Vemula, S. R.; Cook, G. R. Merging C−H bond functionalization with amide alcoholysis: En route to 2-amino-pyridines. *ACS Catal.* **2016**, *6*, 3531−3536.
(42) Gómez-Gallego, M.; Sierra, M. A. Kinetic isotope effects in the study of organometallic reaction mechanisms. *Chem. Rev.* **2011**, *111*, 4857−4963.
(43) Xu, L.-M.; Li, B.-J.; Yang, Z.; Shi, Z.-J. Organopalladium(IV) chemistry. *Chem. Soc. Rev.* **2010**, *39*, 712−733.
(44) Sehnal, P.; Taylor, R. J. K.; Fairlamb, I. J. S. Emergence of palladium(IV) chemistry in synthesis and catalysis. *Chem. Rev.* **2010**, *110*, 824−889.
(45) Racowski, J. M.; Ball, N. D.; Sanford, M. S. C−H bond activation at palladium(IV) centers. *J. Am. Chem. Soc.* **2011**, *133*, 18022−18025.
(46) Martínez-Martínez, A.-J.; Chicote, M.-T.; Bautista, D.; Vicente, J. Synthesis of Palladium(II), -(III), and -(IV) complexes with acyclic diaminocarbene ligands. *Organometallics* **2012**, *31*, 3711−3719.
(47) Malinakova, H. C. Palladium(IV) Complexes as Intermediates in Catalytic and Stoichiometric Cascade Sequences Providing Complex Carbocycles and Heterocycles. In *Higher Oxidation State Organopalladium and Platinum Chemistry*, Topics in Organometallic Chemistry; Springer: Berlin/Heidelberg, 2011; Vol. 35, pp 85−109.
(48) Park, H.; Verma, P.; Hong, K.; Yu, J.-Q. Controlling Pd(IV) Reductive elimination pathways enables Pd(II)-catalyzed enantioselective C(Sp3)−H Fluorination. *Nat. Chem.* **2018**, *10*, 755−762.
(49) Vicente, J.; Arcas, A.; Juliá-Hernández, F.; Bautista, D. Synthesis of a palladium(IV) complex by oxidative addition of an aryl halide to palladium(ii) and its use as precatalyst in a C-C coupling reaction. *Angew. Chem., Int. Ed.* **2011**, *50*, 6896−6899.
(50) Iosub, A. V.; Stahl, S. S. Palladium-catalyzed aerobic oxidative dehydrogenation of cyclohexenes to substituted arene derivatives. *J. Am. Chem. Soc.* **2015**, *137*, 3454−3457.
(51) Wang, L.; Jiang, K. C.; Zhang, N.; Zhang, Z. H. Rhodium-catalyzed synthesis of isoquinolino[1,2-b]quinazolines via C−H annulation in biomass-derived γ-valerolactone. *Asian J. Org. Chem.* **2021**, *10*, 1671−1674.
(52) Marcone, J. E.; Moloy, K. G. kinetic study of reductive elimination from the complexes (diphosphine)Pd(R)(CN). *J. Am. Chem. Soc.* **1998**, *120*, 8527−8528.
(53) Dupont, J.; Consorti, C. S.; Spencer, J. The Potential of palladacycles: More than just precatalysts. *Chem. Rev.* **2005**, *105*, 2527−2572.
(54) Zhao, Q.; Meng, G.; Nolan, S. P.; Szostak, M. N-Heterocyclic carbene complexes in C−H activation reactions. *Chem. Rev.* **2020**, *120*, 1981−2048.
(55) Huynh, H. V. Electronic properties of N-heterocyclic carbenes and their experimental determination. *Chem. Rev.* **2018**, *118*, 9457−9492.
(56) De Risi, C.; Brandolese, A.; Di Carmine, G.; Ragno, D.; Massi, A.; Bortolini, O. Oxidative N-heterocyclic carbene catalysis. *Chem. - Eur. J.* **2023**, *29*, No. e202202467, DOI: 10.1002/chem.202202467.
(57) Díez-González, S.; Nolan, S. P. Stereoelectronic parameters associated with n-heterocyclic carbene (nhc) ligands: a quest for understanding. *Coord. Chem. Rev.* **2007**, *251*, 874−883.
(58) Gómez-Suárez, A.; Nelson, D. J.; Nolan, S. P. Quantifying and understanding the steric properties of N-heterocyclic carbenes. *Chem. Commun.* **2017**, *53*, 2650−2660.
(59) Xu, S.; Yao, H.; Qiu, Y.; Zhou, M.; Li, D.; Wu, L.; Yang, D.-H.; Chen, Z.-S.; Xu, J. Discovery of novel polycyclic heterocyclic derivatives from evodiamine for the potential treatment of triple-negative breast cancer. *J. Med. Chem.* **2021**, *64*, 17346−17365.
(60) Alagarsamy, V.; Chitra, K.; Saravanan, G.; Solomon, V. R.; Sulthana, M. T.; Narendhar, B. An overview of quinazolines: pharmacological significance and recent developments. *Eur. J. Med. Chem.* **2018**, *151*, 628−685.
(61) Bansal, R.; Malhotra, A. Therapeutic Progression of quinazolines as targeted chemotherapeutic agents. *Eur. J. Med. Chem.* **2021**, *211*, No. 113016.
(62) Strohfeldt, K.; Tacke, M. Bioorganometallic fulvene-derived titanocene anti-cancer drugs. *Chem. Soc. Rev.* **2008**, *37*, 1174−1187.
(63) McMorris, T. C. Discovery and development of sesquiterpenoid derived hydroxymethylacylfulvene: A new anticancer drug. *Bioorg. Med. Chem.* **1999**, *7*, 881−886.
(64) Sirignano, E.; Pisano, A.; Caruso, A.; Saturnino, C.; Sinicropi, M.; Lappano, R.; Botta, A.; Iacopetta, D.; Maggiolini, M.; Longo, P. different 6-aryl-fulvenes exert anti-proliferative effects on cancer cells. *Anti-Cancer Agents Med. Chem.* **2015**, *15*, 468−474.
(65) Satpute, D. P.; Shirwadkar, U.; Tharalla, A. K.; Shinde, S. D.; Vaidya, G. N.; Joshi, S.; Vatsa, P. P.; Jain, A.; Singh, A. A.; Garg, R.; Mandoli, A.; Kumar, D. discovery of fluorinated 2-styryl 4(3H)-quinazolinone as potential therapeutic hit for oral cancer. *Bioorg. Med. Chem.* **2023**, *81*, No. 117193.
(66) Elwaie, T. A.; Abbas, S. E.; Aly, E. I.; George, R. F.; Ali, H.; Kraiouchkine, N.; Abdelwahed, K. S.; Fandy, T. E.; El Sayed, K. A.; Abd Elmageed, Z. Y.; Ali, H. I. HER2 Kinase-Targeted breast cancer therapy: design, synthesis, and in vitro and in vivo evaluation of novel lapatinib congeners as selective and potent her2 inhibitors with favorable metabolic stability. *J. Med. Chem.* **2020**, *63*, 15906−15945.
(67) Zhang, K.; Lai, F.; Lin, S.; Ji, M.; Zhang, J.; Zhang, Y.; Jin, J.; Fu, R.; Wu, D.; Tian, H.; Xue, N.; Sheng, L.; Zou, X.; Li, Y.; Chen, X.; Xu, H. Design, synthesis, and biological evaluation of 4-methyl quinazoline derivatives as anticancer agents simultaneously targeting phosphoinositide 3-kinases and histone deacetylases. *J. Med. Chem.* **2019**, *62*, 6992−7014.
(68) Hao, C.; Zhao, F.; Song, H.; Guo, J.; Li, X.; Jiang, X.; Huan, R.; Song, S.; Zhang, Q.; Wang, R.; Wang, K.; Pang, Y.; Liu, T.; Lu, T.; Huang, W.; Wang, J.; Lin, B.; He, Z.; Li, H.; Li, F.; Zhao, D.; Cheng, M. Structure-based design of 6-chloro-4-aminoquinazoline-2-carboxamide derivatives as potent and selective p21-activated kinase 4 (PAK4) inhibitors. *J. Med. Chem.* **2018**, *61*, 265−285.
(69) Liu, F.; Chen, X.; Allali-Hassani, A.; Quinn, A. M.; Wigle, T. J.; Wasney, G. A.; Dong, A.; Senisterra, G.; Chau, I.; Siarheyeva, A.; Norris, J. L.; Kireev, D. B.; Jadhav, A.; Herold, J. M.; Janzen, W. P.; Arrowsmith, C. H.; Frye, S. V.; Brown, P. J.; Simeonov, A.; Vedadi, M.; Jin, J. Protein lysine methyltransferase G9a inhibitors: design, synthesis, and structure activity relationships of 2,4-diamino-7-aminoalkoxy-quinazolines. *J. Med. Chem.* **2010**, *53*, 5844−5857.
(70) Liang, Z.; Wang, Y.; Zhang, H.; Deng, J.; Lei, F.; Li, J.; Shi, T.; Wang, S.; Li, R.; Wang, Z. Design, synthesis and bioactivity evaluation of favorable evodiamine derivative scaffold for developing cancer therapy. *Eur. J. Med. Chem.* **2022**, *239*, No. 114530.

(71) Catanzaro, E.; Betari, N.; Arencibia, J. M.; Montanari, S.; Sissi, C.; De Simone, A.; Vassura, I.; Santini, A.; Andrisano, V.; Tumiatti, V.; De Vivo, M.; Krysko, D. V.; Rocchi, M. B. L.; Fimognari, C.; Milelli, A. Targeting topoisomerase II with trypthantrin derivatives: discovery of 7-((2-(dimethylamino)ethyl)amino)indolo[2,1-b]-quinazoline-6,12-dione as an antiproliferative agent and to treat cancer. *Eur. J. Med. Chem.* **2020**, *202*, No. 112504.
(72) Marzaro, G.; Coluccia, A.; Ferrarese, A.; Brun, P.; Castagliuolo, I.; Conconi, M. T.; La Regina, G.; Bai, R.; Silvestri, R.; Hamel, E.; Chilin, A. Discovery of Biarylaminoquinazolines as novel tubulin polymerization inhibitors. *J. Med. Chem.* **2014**, *57*, 4598−4605.
(73) Hour, M.-J.; Huang, L.-J.; Kuo, S.-C.; Xia, Y.; Bastow, K.; Nakanishi, Y.; Hamel, E.; Lee, K.-H. 6-Alkylamino- and 2,3-Dihydro-3′-methoxy-2-phenyl-4-quinazolinones and related compounds: their synthesis, cytotoxicity, and inhibition of tubulin polymerization. *J. Med. Chem.* **2000**, *43*, 4479−4487.
(74) Peng, F.-W.; Xuan, J.; Wu, T.-T.; Xue, J.-Y.; Ren, Z.-W.; Liu, D.-K.; Wang, X.-Q.; Chen, X.-H.; Zhang, J.-W.; Xu, Y.-G.; Shi, L. Design, synthesis and biological evaluation of N-phenylquinazolin-4-amine hybrids as dual inhibitors of VEGFR-2 and HDAC. *Eur. J. Med. Chem.* **2016**, *109*, 1−12.
(75) Yao, H.; Ji, M.; Zhu, Z.; Zhou, J.; Cao, R.; Chen, X.; Xu, B. Discovery of 1-substituted benzyl-quinazoline-2,4(1H,3H)-dione derivatives as novel poly(ADP-Ribose)polymerase-1 inhibitors. *Bioorg. Med. Chem.* **2015**, *23*, 681−693.
(76) Montero, P. H.; Patel, S. G. Cancer of the oral cavity. *Surg. Oncol. Clin. N. Am.* **2015**, *24*, 491−508.
(77) Cancer Today - CANCER FACT SHEETS. https://gco.iarc.fr/today/fact-sheets-cancers (accessed December 11, 2023).
(78) Hartner, L. Chemotherapy for oral cancer. *Dent. Clin. North Am.* **2018**, *62*, 87−97.
(79) Gioanni, J.; Fischel, J.-L.; Lambert, J.-C.; Demard, F.; Mazeau, C.; Zanghellini, E.; Ettore, F.; Formento, P.; Chauvel, P.; Lalanne, C.-M.; Courdi, A. Two new human tumor cell lines derived from squamous cell carcinomas of the tongue: establishment, characterization and response to cytotoxic treatment. *Eur. J. Cancer Clin. Oncol.* **1988**, *24*, 1445−1455.
(80) Hanahan, D. Hallmarks of cancer: New dimensions. *Cancer Discovery* **2022**, *12*, 31−46.
(81) Hanahan, D.; Weinberg, R. A. Hallmarks of cancer: The next generation. *Cell* **2011**, *144*, 646−674.
(82) Liang, C.-C.; Park, A. Y.; Guan, J.-L. *In vitro* scratch assay: A Convenient and inexpensive method for analysis of cell migration *in vitro*. *Nat. Protoc.* **2007**, *2*, 329−333.
(83) Geraci, F.; Saha, I.; Bianchini, M. Editorial: RNA-Seq Analysis: Methods, applications and challenges. *Front. Genet.* **2020**, *11*, 220.

https://doi.org/10.1021/jacsau.4c00802
JACS Au 2024, 4, 4474−4487